JOURNAL OF NATURAL PRODUCTS

Article

pubs.acs.org/jnp

Phaeosphaerins A−F, Cytotoxic Perylenequinones from an Endolichenic Fungus, *Phaeosphaeria* sp.

Gang Li,[†,⊥] Haiying Wang,[‡,⊥] Rongxiu Zhu,[§] Lingmei Sun,[†] Lining Wang,[†] Ming Li,[‡] Yaoyao Li,[†] Yongqing Liu,[†] Zuntian Zhao,*[,‡] and Hongxiang Lou*[,†]

[†]Department of Natural Products Chemistry, School of Pharmaceutical Sciences, Shandong University, No. 44 West Wenhua Road, Jinan 250012, People's Republic of China

[‡]College of Life Sciences, Shandong Normal University, No. 88 East Wenhua Road, Jinan 250014, People's Republic of China

[§]School of Chemistry and Chemical Engineering, Shandong University, No. 27 Shanda Nanlu, Jinan 250100, People's Republic of China

Supporting Information

ABSTRACT: Six novel phototoxins, phaeosphaerins A−F (**1**−**6**), together with six known perylenequinones were isolated from an endolichenic fungus *Phaeosphaeria* sp. Their structures were determined unequivocally on the basis of comprehensive analysis of MS and NMR data as well as electronic circular dichroism calculations. These toxins kill cancer cells in vitro with accumulation in lysosomes, and the killing effects were potently intensified in the presence of light.

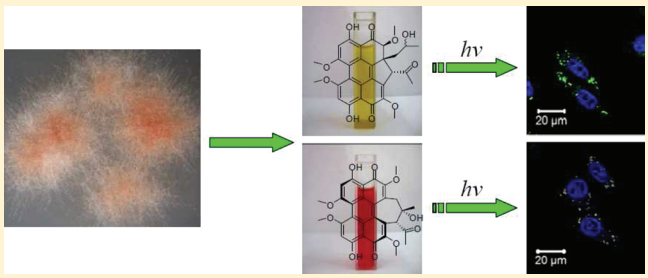

A limited number of natural perylenequinonoid pigments (PQPs) have been found, mainly confined to fungi within the Ascomycota phylum.[1] PQPs absorb light energy and are then transformed to electronically excited triplet states, which can react with oxygen by an electron transfer reaction or energy transfer mechanism to generate extremely cytotoxic reactive oxygen species (ROS).[2] Due to outstanding light-induced biological activities, perylenequinones are attractive cytotoxic agents for investigations.[3]

We report here the discovery and cytotoxic activity of six novel perylenequinones, phaeosphaerins A−F (**1**−**6**; Chart 1). They were obtained from an endolichenic fungus, *Phaeosphaeria* sp. (GenBank: HQ324780), occurring in the lichen *Heterodermia obscurata* (Nyl.) Trevis collected from Yunnan, People's Republic of China. Six known biosynthetically related red perylenequinones, hypocrellins A and C (**7**, **8**),[4] elsinochromes A−C (**9**−**11**),[5] and (+)-calphostin D (**12**),[6] were also afforded. The unusual α,β-unsaturated ketones present in phaeosphaerins A−F (**1**−**6**) resulted in their yellow coloration. Cytotoxicity evaluation using human tumor cells revealed that these pigments kill the cells with accumulation in the lysosomes, and the killing effects can be potently intensified upon light irradiation.

RESULTS AND DISCUSSION

Phaeosphaerin A (**1**), a yellow solid, has the molecular formula $C_{30}H_{26}O_{10}$ as determined by HRESIMS and ^{13}C NMR data, revealing 18 degrees of unsaturation. Detailed analysis of ^{1}H, ^{13}C, and HSQC NMR spectra of **1** (Table 1) revealed the presence of two exchangeable protons, six methyls (four oxygenated), one methylene, two methines (one oxygenated), two quaternary carbons (one ketal carbon), 16 aromatic/olefinic carbons (including five oxygenated carbons and two aromatic methine carbons), and three carbonyl carbons including one α,β-unsaturated ketone, one quinone carbonyl, and one keto carbonyl group. These data accounted for all ^{1}H and ^{13}C NMR resonances and indicated a perylenequinone skeleton with seven rings.[4−6] Interpretation of $^{1}H-^{1}H$ COSY NMR data identified the connection of C-14−C-15−C-16. HMBC correlations from H-14α (δ_H 2.67) to C-1 (δ_C 64.5) and C-2 (δ_C 103.3), from H-14β (δ_H 1.84) to C-1a (δ_C 140.3), and from H_3-18 (δ_H 2.68) to C-13 (δ_C 56.2) and C-17 (δ_C 206.5) established the connection of C-1 to C-1a, C-2, and C-14 and the link of an acetyl group to C-13 (δ_H 5.33). The striking feature of **1** was a C-1/C-13 linkage, which was verified by the detailed HMBC correlations of H-13/C-1, H-13/C-2, H-13/C-11, H-13/C-12, and H-13/C-14 (Figure 1). The remaining one degree of unsaturation and the chemical shifts of C-2 and C-15 (δ_C 74.9) indicated that C-2 and C-15 were both attached to the same oxygen atom to form a tetrahydrofuran ring,[7] which was consistent with its molecular formula. Accordingly, the planar structure of compound **1** was unambiguously established as depicted.

The relative configuration of **1** was assigned by analysis of coupling constants of the protons and its NOESY data. In the NOESY spectrum, H-13 was correlated only to H_3-18 without H-14α, which indicated that H-13 and the methoxy at C-2 were in the same orientation (α-configuration). The large coupling

Received: July 24, 2011
Published: January 25, 2012

Chart 1. Structures of Compounds 1−12

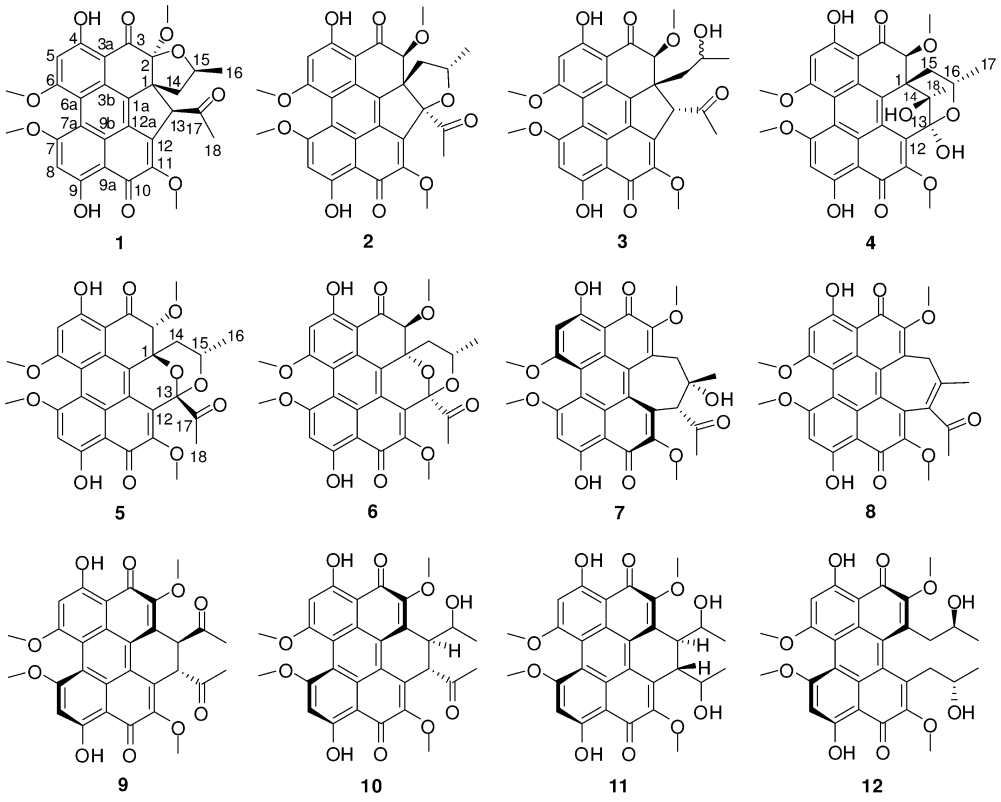

constant (J = 10.2 Hz) between H-14β and H-15 and the strong NOESY correlation of H-14β with H_3-16 lead to assignment of a β-configuration for Me-16. Moreover, the helical perylene core was characterized by two equilibrating atropisomers (P and M in 4:1 ratio for the Boltzmann distribution, Figure 2),[8] as indicated by the calculated energy barrier and energy gap (Experimental Section).

For phaeosphaerin B (**2**), a yellow solid, HRESIMS and ^{13}C NMR spectroscopy established the same molecular formula of $C_{30}H_{26}O_{10}$ as **1**. Analysis of its ^{1}H, ^{13}C, and HSQC NMR spectra (Table 1) revealed similar structural features to those of **1**, except for the absence of H-13 (δ_H 5.33) and the downfield shift of H-2 (δ_H 4.32) in the ^{1}H NMR spectrum of **2**. In the ^{13}C NMR spectrum, the chemical shifts of the C-2 (δ_C 82.7 ppm in **2**; δ_C 103.3 ppm in **1**) and C-13 (δ_C 98.7 ppm in **2**; δ_C 56.2 ppm in **1**) were also different. The analysis above indicated that one oxygen atom attached to C-2 in a five-membered ring of **1** was now connected to C-13 in **2**, which was supported by comprehensive analysis of the HMBC spectrum of **2** (Figure 1).

Phaeosphaerin C (**3**) was also obtained as a yellow solid with a molecular formula of $C_{30}H_{28}O_{10}$, as determined by the same strategy as above. The ^{1}H NMR data of compound **3** (Table 1) were close to those of **2** except for an additional proton signal arising from C-13 (δ_H 4.98). Analysis of the ^{13}C NMR and HSQC spectra revealed the significantly upfield shift of C-13 from δ_C 98.7 in **2** to 60.8 ppm in **3** (Table 1). Detailed HMBC correlations of H-13 to C-1 (δ_C 58.6), C-1a (δ_C 144.8), C-12 (δ_C 138.9), C-12a (δ_C 129.4), C-14 (δ_C 46.8), C-17 (δ_C 207.0), and C-18 (δ_C 33.3) also indicated the location of H-13 and determined the connection of C-13 to C-1, C-12, and C-17 (Figure S24). Consequently, the analysis above suggested a disconnection of the ether linkage in **2** between C-13 and C-15, and the planar structure of compound **3** was thus determined.

Phaeosphaerin D (**4**) was an orange solid. HRESIMS and ^{13}C NMR spectra determined its molecular formula as $C_{30}H_{28}O_{11}$. Analysis of the ^{1}H, ^{13}C, and HSQC NMR data of **4** (Table 1) revealed compound **4** had a perylenequinone framework similar to **3**. HMBC correlations from 13-OH (δ_H 7.02) to C-12 (δ_C 133.1), C-13 (δ_C 97.5), and C-14 (δ_C 73.4) and correlations from 14-OH (δ_H 4.54) to C-13, C-14, and C-1 (δ_C 48.9) established the connection of C-12−C-13−C-14−C-1 (Figure 1). The methyl at C-14 was assigned by the HMBC correlations of H_3-18 with C-1, C-13, and C-14. The chemical shifts of C-13 and C-16 (δ_C 65.9) suggested that C-13 and C-16 were attached to the same oxygen atom to meet the degrees of unsaturation requirement.

Phaeosphaerin E (**5**) was obtained as a yellow solid. A molecular formula of $C_{30}H_{26}O_{11}$ (18 degrees of unsaturation) was assigned for **5** from the HRESIMS and NMR data. Analysis of the ^{1}H, ^{13}C, and HSQC data of **5** (Table 1) indicated that compound **5** was also a novel perylenequinone derivative. The HMBC correlations from H_3-18 to C-13 and C-17 located an acetyl group at C-13 (Figure 1). Considering the ketal carbon at C-13 (δ_C 96.0) and the downfield shifts for signals of C-1 (δ_C 75.3) and C-15 (δ_C 66.3), the presence of an ether linkage between C-1 and C-13 and the oxygen bridge between C-13 and C-15 were revealed and the basic planar structure of **5** was determined.

Finally, the most remarkable finding was that phaeosphaerin F (**6**) had the same planar structure as **5**, which was verified by the 1D and 2D NMR data (Table 1 and Figure S63) but a CD trace opposite that of **5** (Figures S61 and S74).

The relative configurations of phaeosphaerins B−F (**2**−**6**) were also assigned by analysis of ^{1}H−^{1}H coupling constants

dx.doi.org/10.1021/np200614h | J. Nat. Prod. 2012, 75, 142−147

Table 1. ^{1}H and ^{13}C NMR Data for Compounds 1−6

	1		2		3		4		5		6	
position	δ_C, mult.[a]	δ_H, mult.[b] (J in Hz)	δ_C, mult.[a]	δ_H, mult.[b] (J in Hz)	δ_C, mult.[a]	δ_H, mult.[b] (J in Hz)	δ_C, mult.[a]	δ_H, mult.[b] (J in Hz)	δ_C, mult.[a]	δ_H, mult.[b] (J in Hz)	δ_C, mult.[a]	δ_H, mult.[b] (J in Hz)
1	64.5, C		68.4, C		58.6, C		48.9, C		75.3, C		77.0, C	
1a	140.3, C		140.9, C		144.8, C		136.5, C		135.7, C		133.0, C	
2	103.3, C		82.7, CH	4.32, s	85.2, CH	4.66, s	83.3, CH	4.71, s	85.1, CH	4.55, s	84.9, CH	4.56, s
3	197.2, C		200.3, C		200.1, C		198.3, C		196.4, C		196.6, C	
3a	103.0, C		105.0, C		104.7, C		102.4, C		103.7, C		103.3, C	
3b	126.9, C		127.8, C		127.4, C		124.3, C		126.0, C		126.4, C	
4	165.3, C		162.3, C		162.3, C		164.2, C		164.6, C		164.6, C	
5	100.8, CH	6.77, s	100.7, CH	6.73, s	100.8, CH	6.74, s	100.6, CH	6.75, s	100.4, CH	6.76, s	100.5, CH	6.76, s
6	165.6, C		165.6, C		165.7, C		164.4, C		164.8, C		164.7, C	
6a	115.3, C		115.3, C		115.4, C		115.9, C		115.3, C		115.3, C	
7	166.3, C		165.9, C		165.7, C		166.4, C		166.2, C		166.3, C	
7a	112.1, C		112.2, C		112.3, C		112.8, C		113.0, C		112.9, C	
8	100.1, CH	6.78, s	100.1, CH	6.80, s	100.1, CH	6.79, s	99.5, CH	6.79, s	99.6, CH	6.77, s	99.7, CH	6.79, s
9	167.3, C		167.7, C		167.5, C		171.2, C		170.5, C		170.6, C	
9a	108.0, C		108.5, C		108.4, C		107.0, C		107.7, C		107.7, C	
9b	123.4, C		122.9, C		123.5, C		123.8, C		125.1, C		123.7, C	
10	185.2, C		185.0, C		184.7, C		179.9, C		181.6, C		181.5, C	
11	148.5, C		148.5, C		148.3, C		150.9, C		146.8, C		147.7, C	
12	139.4, C		138.1, C		138.9, C		133.1, C		129.2, C		127.5, C	
12a	130.1, C		130.0, C		129.4, C		127.7, C		118.3, C		122.7, C	
13	56.2, CH	5.33, s	98.7, C		60.8, CH	4.98, s	97.5, C		96.0, C		96.1, C	
14α	42.2, CH_2	2.67, br s	38.3, CH_2	2.32, t (12.0)	46.8, CH_2	2.19, dd (15.0, 9.0); 1.56, d (15.0)	73.4, C		37.4, CH_2	2.67, dd (13.2, 4.2)	34.3, CH_2	2.49, dd (13.2, 12.0)
14β		1.84, dd (14.1, 10.2)		1.88, dd (12.0, 4.2)						1.45, dd (13.2, 10.2)		1.43, dd (13.2, 2.4)
15α	74.9, CH	4.22, br s	74.7, CH	3.83, br s	64.7, CH	3.81, br s	31.8, CH_2	2.64, t (13.2)	66.3, CH	4.38, br s	64.9, CH	3.73, br s
15β								1.42, dd (13.2, 3.0)				
16	22.2, CH_3	1.31, d (6.0)	19.1, CH_3	1.36, d (5.4)	24.5, CH_3	1.03, d (6.6)	65.9, CH	3.30, br s	20.6, CH_3	1.16, d (6.6)	21.2, CH_3	1.20, d (6.0)
17	206.5, C		209.9, C		207.0, C		20.9, CH_3	1.14, d (6.0)	202.0, C		201.7, C	
18	32.7, CH_3	2.68, s	28.1, CH_3	2.65, s	33.3, CH_3	2.65, s	21.0, CH_3	1.40, s	25.2, CH_3	2.49, s	24.9, CH_3	2.52, s
2-OMe	53.9, CH_3	3.57, s	60.2, CH_3	3.59, s	60.8, CH_3	3.65, s	60.9, CH_3	3.87, s	62.0, CH_3	3.82, s	62.1, CH_3	3.81, s
6-OMe	56.3, CH_3	4.12, s	56.4, CH_3	4.10, s	56.4, CH_3	4.10, s	56.5, CH_3	4.07, s	56.4, CH_3	4.09, s	56.4, CH_3	4.09, s
7-OMe	56.4, CH_3	4.11, s	56.4, CH_3	4.13, s	56.4, CH_3	4.12, s	56.4, CH_3	4.12, s	56.4, CH_3	4.11, s	56.4, CH_3	4.12, s
11-OMe	59.8, CH_3	4.03, s	60.3, CH_3	4.10, s	60.2, CH_3	4.10, s	62.3, CH_3	4.17, s	60.5, CH_3	4.00, s	60.1, CH_3	4.02, s
4-OH		12.38, s		11.43, s		11.39, s		12.97, s		12.80, s		12.86, s
9-OH		13.62, s		13.75, s		13.71, s		15.45, s		15.08, s		15.10, s
13-OH								7.02, s				
14-OH								4.54, s				

[a]Recorded at 150 MHz; ^{13}C multiplicities were determined by HSQC experiment. [b]Recorded at 600 MHz.

dx.doi.org/10.1021/np200614h | J. Nat. Prod. 2012, 75, 142–147

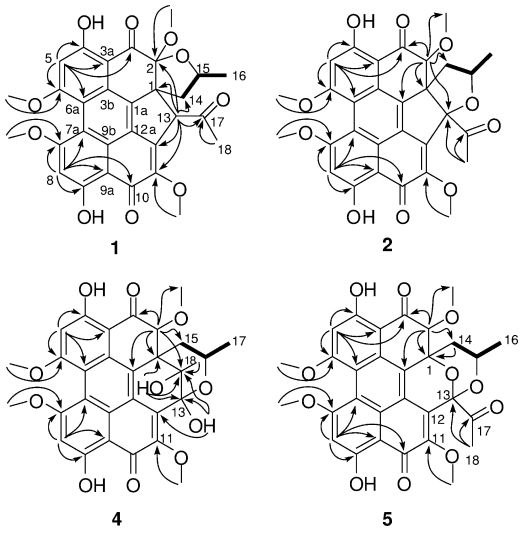

Figure 1. Key HMBC (arrows) and ^{1}H–^{1}H COSY correlations (bold) of **1**, **2**, **4**, and **5**.

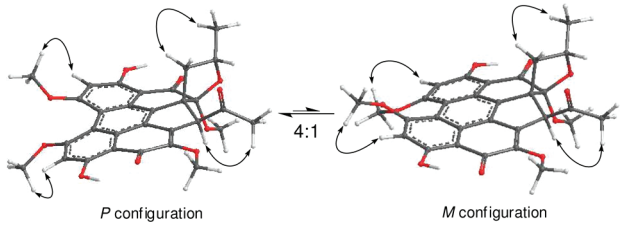

Figure 2. Key NOESY correlations and atropisomeric forms (*P* and *M*) of **1**.

and their NOESY data (Figures S12, S25, S38, S51, and S64). By application of quantum-chemical calculations of electronic circular dichroism spectra (ECD) using time-dependent density functional theory (TDDFT),[9] the absolute structures of all these six phaeosphaerins were finally determined. To determine the absolute configuration of phaeosphaerin A (**1**), the Boltzmann-averaged ECD spectra from all the possible configurations of **1** were used to compare with the experimental CD data. We found that the predicted and experimental ECD spectra were in good agreement (Figure 3). Accordingly, the

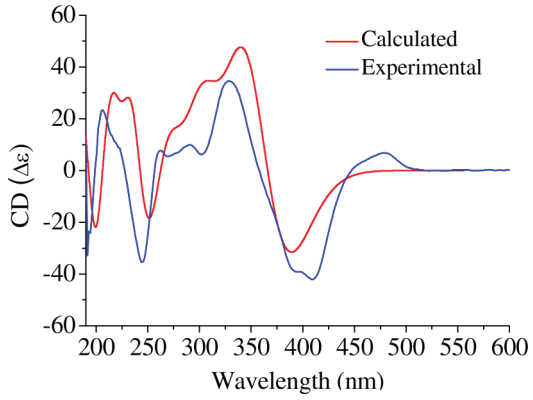

Figure 3. Experimental ECD (blue) and suitable calculated ECD (red) of **1**.

absolute configuration of **1** was determined as 1*R*, 2*S*, 13*S*, and 15*S*. The same method was adapted for the absolute configuration assignments of phaeosphaerins B–F (**2**–**6**) (Figures S22, S35, S48, S61, and S74).

In our ongoing efforts to find natural compounds for treating prostate cancer,[10] compounds **1**–**6** were evaluated for cytotoxicity against PC3, DU145, and LNCaP cell lines using the MTT assay (Table 2). Confocal observations revealed that

Table 2. Cytotoxic Activities of Compounds against Three Cancer Cell Lines[a]

	IC_{50} (μM)[a]		
compound	PC3[b]	DU145[b]	LNCaP[b]
1	5.84 ± 0.06	10.77 ± 0.15	10.76 ± 0.03
2	2.42 ± 0.13	9.54 ± 0.27	2.67 ± 0.27
3	6.11 ± 0.12	15.21 ± 0.10	14.35 ± 0.10
4	9.74 ± 0.03	20.19 ± 0.13	24.92 ± 0.08
5	5.25 ± 0.13	16.25 ± 0.16	10.11 ± 0.16
6	5.45 ± 0.23	16.66 ± 0.13	11.84 ± 0.13
adriamycin	19.51 ± 1.04	23.48 ± 3.11	16.02 ± 2.56

[a]The results are means ± standard deviation of three independent replicates. [b]Human prostate cancer cell lines.

both yellow pigment **3** and red pigment **7** accumulated in lysosomes in tumor cells (Figure S82).

Phototoxic activities of phaeosphaerin C (**3**) and hypocrellin A (**7**) to human K562 cells were also assessed using a modified MTT assay[3d] (Table 3). The above results suggested that the

Table 3. Phototoxic Activities of Compounds 3 and 7 against K562 Cells[a]

	IC_{50} (μM)[a]	
	3	**7**
no light[b]	19.49 ± 0.35	7.47 ± 0.37
light[b]	7.08 ± 0.17	0.55 ± 0.03

[a]The results are means ± standard deviation of three independent replicates. [b]The difference of the condition of cell growth.

novel compounds reported here, like other perylenequinones, can also be activated in the presence of light. In addition, the analysis of ROS generation and the transient absorption spectra (Supporting Information) further confirmed the evidence for photoactivation.

EXPERIMENTAL SECTION

General Experimental Procedures. Optical rotations were measured on a GYROMAT-HP polarimeter, and UV data were recorded on a UV-2450 spectrophotometer (Shimadzu, Japan). Fluorescence spectra were measured with an F-7000 FL spectrophotometer. CD spectra were obtained on a Chirascan spectropolarimeter. IR spectra were recorded using a Thermo Nicolet NEXUS 470 FT-IR spectrometer in KBr discs. The transient absorption spectra were obtained on a Nanosecond laser flash photolysis apparatus, in which the excited laser was a Q-switched Nd:YAG laser (Continuum Surelite, λ: 355 nm), and the signals were collected by an Edinburgh Lp920 and a Tektronix TDS 3012B oscilloscope. Confocal fluorescence microscopy was carried out on a Zeiss LSM 700 confocal microscope. NMR spectra were recorded on a Bruker Avance DRX-600 spectrometer operating at 600 (^{1}H) and 150 (^{13}C) MHz with TMS as internal standard. HRESIMS were carried out on an LTQ-Orbitrap XL. HPLC were performed on an Agilent 1100 G1310A isopump equipped with an Agilent 1100 G1322 degasser, an Agilent 1100 G1314A VWD detector (210 nm), and a ZORBAX SB-C_{18} 5 μm column (9.4 × 250 mm). All solvents used were of analytical grade.

dx.doi.org/10.1021/np200614h | J. Nat. Prod. 2012, 75, 142–147

Silica gel (200−300 mesh; Qingdao Haiyang Chemical Co. Ltd., Qingdao, P. R. China) and Sephadex LH-20 (25−100 μm; Pharmacia Biotek, Denmark) were used for column chromatography. Thin-layer chromatography (TLC) was carried out with glass precoated silica gel GF_{254} plates (Qingdao Haiyang Chemical Co. Ltd.). Compounds were visualized under UV light and by spraying with H_2SO_4/EtOH (1:9, v/v) followed by heating.

Fungal Material. The endolichenic fungus *Phaeosphaeria* sp. (Figure S76) identified by Ming Li based on the nuclear ITS rDNA sequences (GenBank: HQ324780) was isolated from the lichen *Heterodermia obscurata* (Nyl.) Trevis collected from Jiuhe village, Yunnan Province, People's Republic of China. The fungus assigned the accession no. 20081120 was deposited in the lichen lab in the College of Life Sciences, Shandong Normal University, Jinan. The fungal strain was cultured on slants of potato dextrose agar (PDA) at 25 °C for 15 days. Then, the fungus was cultured in five Erlenmeyer flasks (500 mL) each containing 200 mL of PDA to obtain the seed culture. Flask cultures were incubated at 22 °C on a rotary shaker (110 rpm) for seven days. Finally, seed broth (1 mL) was added to 70 Erlenmeyer flasks (500 mL) each containing 200 mL of PDA, and these flasks were maintained at 22 °C for 30 days in a shaker incubator (110 rpm).

Extraction and Isolation. The fermented material was filtered to remove mycelia. The filtrate was concentrated under reduced pressure to 1 L and then extracted with $CHCl_3$ (5 × 1 L). The crude extract (4.0 g) was separated by column chromatography on Si gel eluting with a gradient of petroleum ether (60−90 °C)/Me_2CO from 100:0 to 0:1 (v/v) to give nine fractions (A−I). Fraction C (18 mg) was subjected to a Sephadex LH-20 column ($CHCl_3$/MeOH, 1:1) to obtain three subfractions (C1−C3). Fraction C2 (12 mg) was further separated by Sephadex LH-20 column chromatography using MeOH as eluent, followed by HPLC (MeOH/H_2O, 95:5, 1.8 mL/min) to afford **1** (2.8 mg, t_R = 13.4 min) and **2** (2.0 mg, t_R = 12.6 min). Fraction D (60 mg) was also applied to a Sephadex LH-20 column (MeOH) to provide four subfractions (D1−D4). Further separation of D2 (6 mg) by HPLC (MeOH/H_2O, 87:13, 1.8 mL/min) gave **5** (1.6 mg, t_R = 16.2 min) and **6** (1.8 mg, t_R = 15.3 min). After crystallization from MeOH, subfraction D3 (20 mg) was then purified by HPLC (MeOH/H_2O/MeCN, 60:10:30, 1.8 mL/min) to yield **7** (15.7 mg, t_R = 12.9 min). Fraction E (76 mg) was fractioned by repeated Sephadex LH-20 column chromatography using the same solvent system as described above to give four subfractions (E1−E4). Fraction E2 (10 mg) was separated by HPLC (MeOH/H_2O, 80:20, 1.8 mL/min) to obtain **3** (7.2 mg, t_R = 16.1 min), while fraction E3 (7 mg) afforded **9** (0.9 mg, t_R = 18.4 min) and **8** (1.2 mg, t_R = 21.3 min) after HPLC (MeOH/H_2O, 87:13, 1.8 mL/min). Separation of fraction F (300 mg) following a similar procedure to that used for fraction E gave **4** (HPLC, MeOH/H_2O, 90:10, 1.8 mL/min; 6.8 mg, t_R = 11.5 min) and **12** (HPLC, MeOH/H_2O, 75:25, 1.8 mL/min; 3.2 mg, t_R = 9.0 min). Fraction G (40 mg) was purified by HPLC (MeOH/H_2O, 85:15, 1.8 mL/min) to afford **10** (12.0 mg, t_R = 13.9 min) and **11** (6.7 mg, t_R = 12.0 min).

*Phaeosphaerin A (**1**):* yellow solid; $[\alpha]^{20}_D$ −325.1 (*c* 0.278, $CHCl_3$); UV (MeOH) λ_{max} (log ε) 243 (4.29), 266 (4.27), 408 (4.13) nm; CD (MeOH) 192 (Δε −5.84), 207 (Δε +4.17), 244 (Δε −6.31), 262 (Δε +1.36), 291 (Δε +1.77), 328 (Δε +6.17), 409 (Δε −7.52), 480 (Δε +1.22) nm; IR (KBr) ν_{max} 3419, 2938, 1717, 1626, 1596, 1464, 1392, 1256, 1211, 1162 cm^{-1}; ^1H NMR ($CDCl_3$, 600 MHz) and ^{13}C NMR ($CDCl_3$, 150 MHz), see Table 1; positive ESIMS *m*/*z* (%) 547.3 (100) $[M + H]^+$, 569.3 (80) $[M + Na]^+$; positive HRESIMS *m*/*z* 547.1611 $[M + H]^+$ (calcd for $C_{30}H_{27}O_{10}$, 547.1599).

*Phaeosphaerin B (**2**):* yellow solid; $[\alpha]^{20}_D$ −176.4 (*c* 0.196, $CHCl_3$); UV (MeOH) λ_{max} (log ε) 243 (4.33), 264 (4.29), 408 (4.18) nm; CD (MeOH) 220 (Δε +2.06), 240 (Δε −3.55), 261 (Δε +3.83), 295 (Δε −1.19), 324 (Δε +5.34), 409 (Δε −3.96), 481 (Δε +0.65) nm; IR (KBr) ν_{max} 3435, 2927, 1711, 1636, 1593, 1465, 1392, 1257, 1210, 1159 cm^{-1}; ^1H NMR ($CDCl_3$, 600 MHz) and ^{13}C NMR ($CDCl_3$, 150 MHz), see Table 1; positive ESIMS *m*/*z* (%) 547.5 (100) $[M + H]^+$, 569.4 (35) $[M + Na]^+$; positive HRESIMS *m*/*z* 547.1607 $[M + H]^+$ (calcd for $C_{30}H_{27}O_{10}$, 547.1599).

*Phaeosphaerin C (**3**):* yellow solid; $[\alpha]^{20}_D$ −284.5 (*c* 0.717, $CHCl_3$); UV (MeOH) λ_{max} (log ε) 242 (4.48), 265 (4.46), 407 (4.30) nm; CD (MeOH) 219 (Δε +8.05), 241 (Δε −6.30), 261 (Δε +4.37), 295 (Δε −4.25), 327 (Δε +6.26), 387 (Δε −5.87), 403 (Δε −5.67), 477 (Δε +0.882) nm; IR (KBr) ν_{max} 3462, 2935, 1713, 1634, 1593, 1464, 1392, 1260, 1211, 1165 cm^{-1}; ^1H NMR ($CDCl_3$, 600 MHz) and ^{13}C NMR ($CDCl_3$, 150 MHz), see Table 1; positive ESIMS *m*/*z* (%) 549.4 (95) $[M + H]^+$, 571.4 (100) $[M + Na]^+$; positive HRESIMS *m*/*z* 549.1761 $[M + H]^+$ (calcd for $C_{30}H_{29}O_{10}$, 549.1755).

*Phaeosphaerin D (**4**):* orange solid; $[\alpha]^{20}_D$ −31.2 (*c* 0.675, $CHCl_3$); UV (MeOH) λ_{max} (log ε) 243 (4.57), 267 (4.55), 278 (4.56), 398 (4.37), 419 (4.45), 509 (4.03) nm; CD (MeOH): 222 (Δε −14.47), 247 (Δε +11.13), 274 (Δε +15.43), 315 (Δε −5.64), 400 (Δε +12.43), 423 (Δε +10.53), 493 (Δε −4.11), 520 (Δε −4.75) nm; IR (KBr) ν_{max} 3454, 2934, 1618, 1582, 1436, 1405, 1285, 1211, 1166 cm^{-1}; ^1H NMR ($CDCl_3$, 600 MHz) and ^{13}C NMR ($CDCl_3$, 150 MHz), see Table 1; positive ESIMS *m*/*z* (%) 565.4 (59) $[M + H]^+$, 587.3 (100) $[M + Na]^+$; positive HRESIMS *m*/*z* 565.1716 $[M + H]^+$ (calcd for $C_{30}H_{29}O_{11}$, 565.1704).

*Phaeosphaerin E (**5**):* yellow solid; $[\alpha]^{20}_D$ −219.2 (*c* 0.159, $CHCl_3$); UV (MeOH) λ_{max} (log ε) 244 (4.43), 278 (4.43), 396 (4.20), 415 (4.29) nm; CD (MeOH) 219 (Δε +9.29), 250 (Δε −8.67), 271 (Δε −10.64), 316 (Δε +0.53), 342 (Δε +1.14), 400 (Δε −6.47), 420 (Δε −6.39), 484 (Δε +2.23), 510 (Δε +2.71) nm; IR (KBr) ν_{max} 3436, 2930, 1736, 1629, 1585, 1437, 1399, 1288, 1209, 1158 cm^{-1}; ^1H NMR ($CDCl_3$, 600 MHz) and ^{13}C NMR ($CDCl_3$, 150 MHz), see Table 1; positive ESIMS *m*/*z* (%) 563.3 (100) $[M + H]^+$, 585.3 (55) $[M + Na]^+$; positive HRESIMS *m*/*z* 563.1558 $[M + H]^+$ (calcd for $C_{30}H_{27}O_{11}$, 563.1548).

*Phaeosphaerin F (**6**):* yellow solid; $[\alpha]^{20}_D$ +115.4 (*c* 0.175, $CHCl_3$); UV (MeOH) λ_{max} (log ε) 244 (4.47), 270 (4.45), 276 (4.46), 398 (4.22), 418 (4.32) nm; CD (MeOH) 220 (Δε −11.92), 250 (Δε +12.07), 271 (Δε +14.02), 316 (Δε −1.75), 342 (Δε −1.99), 402 (Δε +9.01), 423 (Δε +8.73), 489 (Δε −2.65), 513 (Δε −3.09) nm; IR (KBr) ν_{max} 3436, 2930, 1737, 1626, 1583, 1438, 1400, 1287, 1210, 1167 cm^{-1}; ^1H NMR ($CDCl_3$, 600 MHz) and ^{13}C NMR ($CDCl_3$, 150 MHz), see Table 1; positive ESIMS *m*/*z* (%) 563.4 (100) $[M + H]^+$, 585.3 (28) $[M + Na]^+$; positive HRESIMS *m*/*z* 563.1555 $[M + H]^+$ (calcd for $C_{30}H_{27}O_{11}$, 563.1548).

Biological Evaluation. Human prostate cancers PC-3, DU145, and LNCaP cells were cultured in RPMI 1640 medium (HyClone) supplemented with 10% FBS (HyClone). The cells were maintained in 5% CO_2 at 37 °C. The 3-(4,5-Dimethylthiazol-2-yl)-2,5-diphenyl-2*H*-tetrazolium bromide (MTT, Sigma) colorimetric assay was used to evaluate cell proliferation in the presence of different chemicals. The cells were seeded in 96-well culture plates and treated with vehicle or desired concentrations of chemicals for a further 24 h. After treatment, cells were incubated at 37 °C with MTT (10 μL/well, 5 mg/mL) for 4 h, and the cell growth response to the chemicals was determined by measuring the absorbance at 570 nm on a plate reader (Bio-Rad, USA). Three replicates were used for each treatment. In order to evaluate the phototoxic activitivies of compounds against K562 cells, the cells were incubated with compounds for 4 h and then irradiated by invisible light for 1000 s in the MTT assay process.

Theory and Calculation Details. The calculations were performed with the Gaussian 03 program package.[11] The semi-empirical AM1 method[12] and a DFT approach,[13] B3LYP/6-31G*, were employed to scan the potential energy surface. The geometries of all ground-state conformations obtained were further optimized at the B3LYP/6-31G* level at 298.15 K, followed by calculations of their harmonic frequency analysis to confirm these minima and then calculations of room-temperature free energies.

Time-dependent density functional theory[9a] at the same level was used to calculate the electronic excitation energies and rotational strengths in the gas phase for the first 30 states. The rotatory strengths were summed and energetically weighted following the Boltzmann statistics, and the final ECD spectra were then simulated by overlapping Gaussian functions according to the following

equation.[14]

$$\Delta\varepsilon(E) = \frac{1}{2.297 \times 10^{-39}} \frac{1}{\sqrt{2\pi\sigma}} \times \sum_i \Delta E_{0i} R_{0i} e^{-[(E-\Delta E_{0i})/2\sigma]^2}$$

where σ is the width of the band at $1/e$ height, while ΔE_i and R_i are the excitation energies and rotatory strengths for transition, respectively. σ = 0.1 eV and R_{vel} were used.

For this type of compound, the helical perylene core was characterized by two equilibrating atropisomers (*P* and *M*), which was further confirmed by the followed analysis. From the AM1 scan and DFT geometry optimization, two stable conformers, the *P*-isomer and *M*-isomer, were obtained. We calculated the energy barrier to atropisomerization of *P* and *M* at the B3LYP/6-31G* level and found it was about 11 kcal·mol^{-1}, which indicates that these two isomers can transform into each other and compound **1** exists as an equilibrium mixture of atropisomers at room temperature. The energy gap between *P*- and *M*-isomers was calculated to be about 1.05 kcal·mol^{-1}, which resulted in about 4:1 distribution of *P* and *M* in phaeosphaerin A (**1**).

■ ASSOCIATED CONTENT

Ⓢ Supporting Information

Spectral data of compounds **1**−**6**. This material is available free of charge via the Internet at http://pubs.acs.org.

■ AUTHOR INFORMATION

Corresponding Author

*Fax: +86-531-8838-2019 (H.L.); +86-531-8618-0749 (Z.Z.). E-mail: louhongxiang@sdu.edu.cn (H.L.); ztzhao@sohu.com (Z.Z.).

Author Contributions

⊥These authors contributed equally.

■ ACKNOWLEDGMENTS

This work was financially supported by the National Natural Science Foundation of China (nos. 30925038 and 30730109). We thank Mrs. J. Ren and Mr. B. Ma for the NMR measurements.

■ REFERENCES

(1) (a) Zhou, Z. Y.; Liu, J. K. *Nat. Prod. Rep.* **2010**, *27*, 1531−1570. (b) Mulrooney, C. A.; Morgan, B. J.; Li, X. L.; Kozlowski, M. C. *J. Org. Chem.* **2010**, *75*, 16−29.

(2) (a) Daub, M. E.; Leisman, G. B.; Clark, R. A.; Bowden, E. F. *Proc. Natl. Acad. Sci. U. S. A.* **1992**, *89*, 9588−9592. (b) Daub, M. E.; Ehrenshaft, M. *Annu. Rev. Phytopathol.* **2000**, *38*, 461−490. (c) Daub, M. E.; Herrero, S.; Chung, K. R. *FEMS Microbiol. Lett.* **2005**, *252*, 197−206.

(3) (a) Smirnov, A.; Fulton, D. B.; Andreotti, A.; Petrich, J. W. *J. Am. Chem. Soc.* **1999**, *121*, 7979−1788. (b) O'Brien, E. M.; Morgan, B. J.; Kozlowski, M. C. *Angew. Chem., Int. Ed.* **2008**, *47*, 6877−6880. (c) Morgan, B. J.; Dey, S.; Johnson, S. W.; Kozlowski, M. C. *J. Am. Chem. Soc.* **2009**, *131*, 9413−9425. (d) Zhang, Y.; Xie, J.; Zhang, L. Y.; Li, C.; Chen, H. X.; Gu, Y.; Zhao, J. Q. *Photochem. Photobiol. Sci.* **2009**, *8*, 1676−1682.

(4) Kishi, T.; Tahara, S.; Taniguchi, N.; Tsuda, M.; Tanaka, C.; Takahashi, S. *Planta Med.* **1991**, *57*, 376−379.

(5) (a) Lousberg, R. J. J. C.; Salemink, C. A.; Weiss, U.; Batterham, T. J. *J. Chem. Soc. C* **1969**, 1219−1227. (b) Kurobane, I.; Vining, L. C.; Mcinnes, A. G.; Smith, D. G.; Walter, J. A. *Can. J. Chem.* **1981**, *59*, 422−430. (c) Mebius, H. J.; Krabbendam, H.; Duisenberg, A. J. M. *Acta Crystallogr C.* **1990**, *46*, 267−271.

(6) Morgan, B. J.; Mulrooney, C. A.; O'Brien, E. M.; Kozlowski, M. C. *J. Org. Chem.* **2010**, *75*, 30−43.

(7) Li, E. W.; Tian, R. R.; Liu, S. C.; Chen, X. L.; Guo, L. D.; Che, Y. S. *J. Nat. Prod.* **2008**, *71*, 664−668.

(8) O'Brien, E. M.; Morgan, B. J.; Mulrooney, C. A.; Carroll, P. J.; Kozlowski, M. C. *J. Org. Chem.* **2010**, *75*, 57−68.

(9) (a) Diedrich, C.; Grimme, S. *J. Phys. Chem. A* **2003**, *107*, 2524−2539. (b) Zhang, Y. L.; Ge, H. M.; Zhao, W.; Dong, H.; Xu, Q.; Li, S. H.; Li, J.; Zhang, J.; Song, Y. C.; Tan, R. X. *Angew. Chem., Int. Ed.* **2008**, *47*, 5823−5826.

(10) (a) Liu, H.; Liu, Y. Q.; Liu, Y. Q.; Xu, A. H.; Young, C. Y. F.; Yuan, H. Q.; Lou, H. X. *Chem.-Biol. Interact.* **2010**, *188*, 598−606. (b) Guo, D. X.; Zhu, R. X.; Wang, X. N.; Wang, L. N.; Wang, S. Q.; Lin, Z. M.; Lou, H. X. *Org. Lett.* **2010**, *12*, 4404−4407.

(11) Frisch, M. J.; Trucks, G. W.; Schlegel, H. B.; Scuseria, G. E.; Robb, M. A.; Cheeseman, J. R.; Montgomery, J. A., Jr.; Vreven, T.; Kudin, K. N.; Burant, J. C.; Millam, J. M.; Iyengar, S. S.; Tomasi, J.; Barone, V.; Mennucci, B.; Cossi, M.; Scalmani, G.; Rega, N.; Petersson, G. A.; Nakatsuji, H.; Hada, M.; Ehara, M.; Toyota, K.; Fukuda, R.; Hasegawa, J.; Ishida, M.; Nakajima, T.; Honda, Y.; Kitao, O.; Nakai, H.; Klene, M.; Li, X.; Knox, J. E.; Hratchian, H. P.; Cross, J. B.; Bakken, V.; Adamo, C.; Jaramillo, J.; Gomperts, R.; Stratmann, R. E.; Yazyev, O.; Austin, A. J.; Cammi, R.; Pomelli, C.; Ochterski, J. W.; Ayala, P. Y.; Morokuma, K.; Voth, G. A.; Salvador, P.; Dannenberg, J. J.; Zakrzewski, V. G.; Dapprich, S.; Daniels, A. D.; Strain, M. C.; Farkas, O.; Malick, D. K.; Rabuck, A. D.; Raghavachari, K.; Foresman, J. B.; Ortiz, J. V.; Cui, Q.; Baboul, A. G.; Clifford, S.; Cioslowski, J.; Stefanov, B. B.; Liu, G.; Liashenko, A.; Piskorz, P.; Komaromi, I.; Martin, R. L.; Fox, D. J.; Keith, T.; Al-Laham, M. A.; Peng, C. Y.; Nanayakkara, A.; Challacombe, M.; Gill, P. M. W.; Johnson, B.; Chen, W.; Wong, M. W.; Gonzalez, C.; Pople, J. A. *Gaussian03*, revision A.1; Gaussian, Inc.: Pittsburgh, PA, 2004.

(12) Dewar, M. J. S.; Zoebisch, E. G.; Healy, E. F.; Stewart, J. J. P. *J. Am. Chem. Soc.* **1985**, *107*, 3902−3909.

(13) Becke, A. D. *J. Chem. Phys.* **1993**, *98*, 5648−5652.

(14) Stephens, P. J.; Harada, N. *Chirality* **2010**, *22*, 229−233.